Front. Phys. China (2006) 3: 362－367
DOI 10.1007/s11467-006-0025-9

RESEARCH ARTICLE

DONG Shuai, ZHU Han, LIU Jun-ming

Colossal resistivity change associated with the charge ordered/disordered transition: Monte Carlo study

Abstract Earlier theoretical approaches to manganites mainly stem from magnetic framework in which the electronic transports are thought to be spin-dependent and the double exchange plays a vital role. However, quite a number of experimental observations cannot be explained in the magnetic framework, yet. For example, multiplicate insulator-metal transitions and resistivity reduction induced by perturbations other than magnetic field, such as electric current, are not well understood in this framework. Here we present a comprehensive analysis on the magnetic framework and give a Monte Carlo study on the resistivity of a charge ordered/disordered model without accounting for the spin degree of freedom. The result shows a colossal resistivity change as a resultant of the transition between two types of insulated states. This transition has intrinsic difference from the popular insulated-to-metallic transition in the magnetic framework. The present scenario can be used to explain some experimental facts for electronic transports in manganites, which are not accessible in the magnetic framework.

Keywords manganites, colossal magnetoresistance

PACS numbers 75.47.Lx, 75.47.Gk, 71.30.+h

DONG Shuai, LIU Jun-ming (✉)
Nanjing National Laboratory of Microstructures, Nanjing University, Nanjing 210093, China
E-mail:liujm@nju.edu.cn

ZHU Han
Department of Physics, Princeton University, Princeton, New Jersey 08544, USA

LIU Jun-ming
International Center for Materials Physics, Chinese Academy of Sciences, Shenyang 110016, China

Received May 27, 2006

1 Introduction

Manganites, typical strongly correlated electron systems, have been extensively studied over the last decade because of their colossal magneto-resistance (CMR) effect [1]. The general chemical composition for manganites is $T_{1-x}D_xMnO_3$, with T a trivalent rare earth cation, and D a divalent alkaline earth cation or Pb^{2+}. In mixed-valent manganites, the hopping of $3d$ e_g electrons causes ferromagnetic coupling between localized Mn $3d$ t_{2g} spins, resulting in a significant resistivity reduction under external magnetic field. This is the so called double exchange (DE) mechanism. Quite a number of theoretical approaches proposed to explain the CMR effect and relevant phenomena that are based on the DE mechanism, with additional interactions such as Hund coupling, Jahn-Teller effect, Coulomb repulsion, including antiferromagnetic super-exchange. These approaches are all classified in the magnetic framework. It should be noted that the intrinsic large magnetic field that is required for CMR effect and which causes imbalance between high Curie temperature (T_C) and large magneto-resistance (MR) make the magnetic applications of manganites challenging.

Recent investigations unveiled that manganites are intrinsically inhomogeneous. Phase separation (PS) and percolation were repeatedly observed through experiments [2－4] and were also predicted theoretically [5－10]. Conventional theories in the magnetic framework take this PS scenario into account and emphasize three fundamental facts: first, because of the DE mechanism, ferromagnetic (FM) phase is metallic while antiferromagnetic (AFM) phase and paramagnetic (PM) phase are insulated. Second, the PS structure consists of FM metallic clusters and insulated regions. It is argued that the PS structure on micrometer scale is induced by quenched disorders, in which the percolation of metallic clusters embedded in insulated matrix may occur. Finally, the insulated regions can be partly converted into metallic phase on application of external magnetic field, which is characterized by the raise of temperature T_{IM} for insula-

tor-metal transition (IMT) and enhanced MR effect near T_{IM}. In accordance to the raise in temperature, the Curie temperature (T_C) is raised, too.

Indeed, the magneto-transport behaviors in some large bandwidth manganites, for instance $La_{1-x}Sr_xMnO_3$ (x~0.3) [2], can be reasonably understood in the magnetic framework, while some anomalous properties that are observed in other manganites are not accessible in this framework. First, most manganites are facilitated with charge ordered (CO) states over a broad doping density range below certain temperature $T = T_{CO}$. Although the CO states may be melted under magnetic field [10—12], this field threshold for such a melting condition is large and an appreciable change of resistivity becomes impossible, unless a field beyond this threshold is applied. Such a threshold for $Pr_{0.6}Ca_{0.4}MnO_3$ is ~ 4.2 T at 30 K [12]. These behaviors will not be observable for $La_{2/3}Sr_{1/3}MnO_3$ in which the resistivity response to the magnetic field is nearly linear [13], since no CO state exists in $La_{2/3}Sr_{1/3}MnO_3$. Second, for manganites of intermediate and narrow bandwidth, e.g., $Pr_{1-x}Ca_xMnO_3$, the IMT or colossal reduction of resistivity can be induced by external fluctuations other than magnetic field, such as photon illumination [14—17], electric current [18, 19], and pressure [20, 21]. These phenomena cannot be predicted in the magnetic framework. Third, theoretical investigations [22–27] predicted that the quenched disorder may suppress the charge/lattice ordering and resistivity considerably, while the FM ordering remains less affected. Recent experiments [25] confirmed this prediction: the A-site-disorder in $Pr_{0.6}R_{0.1}Sr_{0.3}MnO_3$ (R=Tb, Y, Ho, and Er) induced by different R-doping indeed causes significant resistivity change, while the measured magnetization (M) as a function of temperature T does not change much. Finally, AFM metallic state was observed in some manganites at a divalent doping x~0.5, e.g., $La_{0.46}Sr_{0.54}MnO_3$ [28] and $Nd_{0.45}Sr_{0.55}MnO_3$ [29], which also is incompatible with the magnetic framework. These anomalous behaviors allow us to appeal for a novel framework as a complementary to the magnetic framework, which will be the objective of the present study.

2 Charge ordered/disordered model

In general, one is allowed to argue that the electronic transport of manganites is determined by both spin correlation and charge correlation. For the spin correlation, due to the DE process, it is known that the nonzero angle between spins of nearest neighboring (NN) Mn cations restrains the e_g electron from hopping. The as-generated spin-dependent resistivity is expressed as ρ_s. upon the magnetism transforms within the PM/FM/AFM. The variation of ρ_s upon magnetic transitions among the PM/FM/AFM states is not very significant. As for the charge correlation, the resistivity due to the charge ordering or disordering, expressed as ρ_c here, can be even more significant. The total resistivity of the system under investigation is $\rho = \rho_s + \rho_c$, if both spin correlation and charge correlation co-occur. Obviously ρ_c depends on the fluctuations of the charge ordered states. That is to say, the variation of the total conductivity does not necessarily correspond to the fluctuations of the spin correlations.

In fact, the charge correlation is more important than spin correlation in terms of the colossal resistivity change, as revealed experimentally. In many cases, the conductivity is independent of the magnetism, although the DE process indeed combines metallic conductance with FM state in a few special cases. To illustrate this idea, a preliminary Monte Carlo (MC) simulation on the electronic transport of a charge ordered/disordered toy model is conducted. Here the spin degree of freedom is discarded, i.e., no spin correlation of electrons is accounted. In this model system, the NN coulomb repulsion represents the sole origin for resistance.

The "spinless" electrons are distributed in a three dimensions (3D) L^3 cubic lattice. The Hamiltonian of the model is:

$$H = \sum_i e\boldsymbol{E}\cdot\boldsymbol{i}n_i + V\sum_{\langle i,j\rangle} n_i n_j + \mu_i n_i \tag{1}$$

where e is the charge unit; E is the biased electric field; $i(j)$ is the location index; n_i indicates the number of electrons on i site; V is the Coulomb repulsion between e_g electrons on NN sites i and j ($\langle i, j\rangle$); μ_i is the chemical potential of e_g electrons on i site. Electrons can hop between the NN sites. But occupation of two electrons on one site is forbidden due to the large on-site Coulomb repulsion (in real manganites, the Hund rule and Jahn-Teller effect gives the same result), so n_i can be either 0 or 1. Here V is taken as the energy term and all other energy parameters are normalized by V.

The MC simulation begins by randomly distributing ~ $L^3/2$ electrons in the L^3 (L=128 in our simulation) sites, corresponding to the half filling manganites. A standard *Metropolis* algorithm is employed. In each step, site i is selected at random. If $n_i = 0$, we stop and initiate the next step. If $n_i = 1$, the electron at site i is assumed to hop to a NN site j, if $n_j = 0$. We calculate the energy difference ΔH of the lattice before and after the assumed hopping. The probability for approving this hopping is p_{ij}:

$$p_{ij} = \exp\left(-\frac{\Delta H}{k_B T}\right) \tag{2}$$

Here, k_B is the Boltzmann constant. We execute the electron hopping to site j according to the probability and then start the next step. In our simulation, the bias field E (taken as 1 in our simulation), which causes the electrical current, is set in x-direction. We run this simulation from high T to low T as a cooling sequence, and evaluate the resistivity as a function of T.

3 Results of Simulation

If the chemical potential μ_i at site i over the whole lattice is set at the same value μ ($\mu = 0$), the ground state of this model system takes the CO state due to the NN Coulomb

repulsion V, as shown in Fig. 1 (a). This is known as a Wigner crystal. In contrast, if some chemical potential disorder which can be generated through various roadmaps is introduced into the lattice, the ground state may deviate from the Wigner crystal. We impose site-dependent fluctuations of the chemical potential onto the lattice with the expectation value $\langle \mu_i \rangle = 0$. It is found that the charge configuration is susceptive to the disorder and the ground state evolves into a charge disordered (CDO) state at low T, as shown in Fig. 1 (b). To characterize the charge ordering degree quantitatively, the average NN charge correlation C is calculated as:

$$C = \frac{1}{N} \sum_{\langle i,j \rangle} n_i n_j \tag{3}$$

Here $N = L^3$ is the number of total sites. The calculated C as a function of T for both the CO and CDO states is shown in Fig. 2. At low T, C goes close to 0 for the Wigner crystal which is a complete CO state, as confirmed in Fig. 2. A rapid decrease of C with decreasing T corresponds to the phase transition. When the disorder is induced, the CO at low T is partially destructed and a CDO state is developed, giving a nonzero C which is larger than that given for the CO state at low T.

The degree of disorder can be scaled by the amplitude of spatial fluctuations of the chemical potential, though $\langle \mu_i \rangle = 0$ is maintained in our simulation. The amplitude is defined as:

$$\sigma^2 = \frac{1}{N} \sum_i \mu_i^2 - \left(\frac{1}{N} \sum_i \mu_i \right)^2 = \frac{1}{N} \sum_i \mu_i^2 \tag{4}$$

with $\langle \mu_i \rangle = \frac{1}{N} \sum_i \mu_i = 0$. The C-T curve shown in Fig. 2 for the CDO state is simulated at $\sigma^2 = 5.972\ 49$. What should be noted here is that the neighbor correlation of μ_i is also taken into account in our simulation. So the site-dependent μ_i is not fully random but correlated with the neighbors, as done in Ref. [7]. A 2D section of the 3D fluctuations of μ_i is shown in Fig. 3, in which the colour blocks implicate the neighbor correlations.

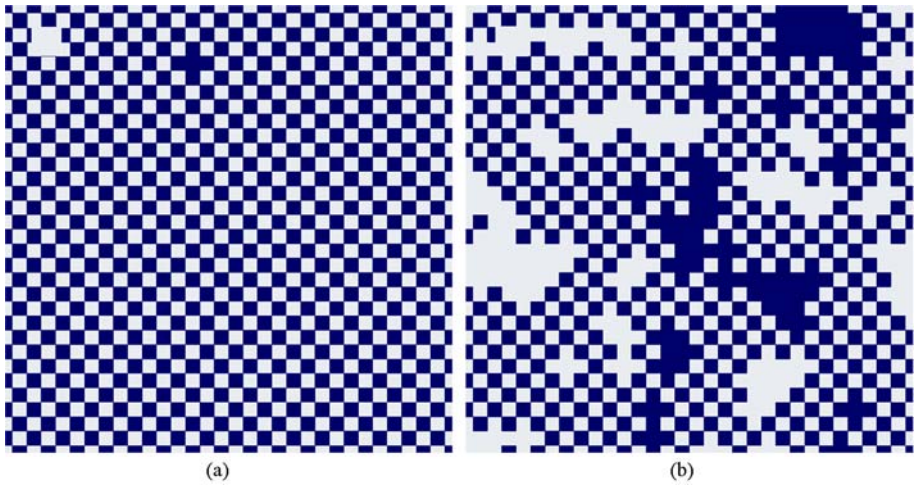

Fig. 1 Snapshot of 2D slices (32×32) cut from the 3D lattice (128×128×128). Electrons occupy the blue sites while the gray sites means holes. (**a**) No disorder and the system develops into a CO state at low $T = 0.175$. (**b**) With disorder, the charge order is partially broken at the same T.

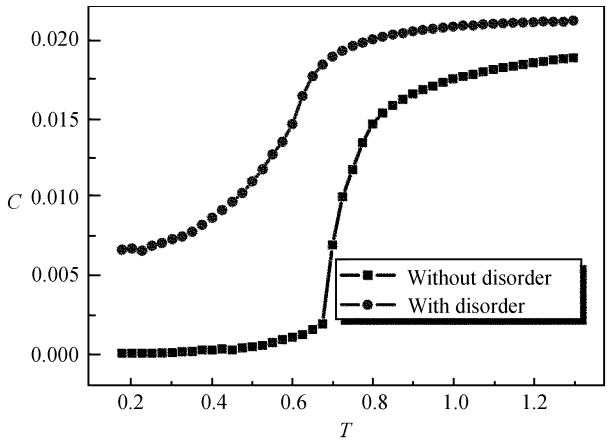

Fig. 2 NN charge correlation C as a function of T for the CO state (σ^2=0, without disorder) and CDO state (σ^2=5.972 49, with disorder).

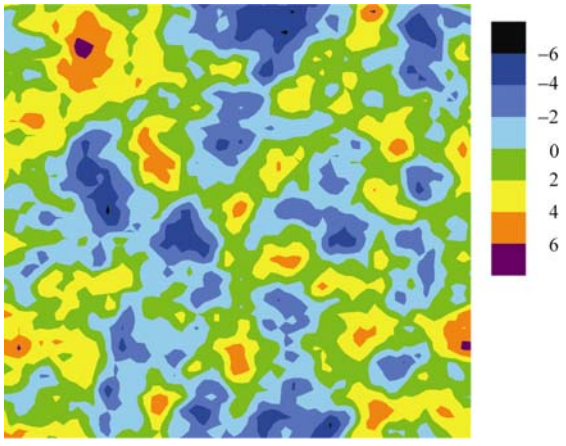

Fig. 3 A 2D (128×128) section of the 3D potential profile μ_i. The neighbour correlation of μ_i is clearly identified by the colour blocks. Here the disorder amplitude σ^2 is 5.972 49.

The resistivity ρ_c as a function of T for $\sigma^2 = 0$ and $\sigma^2 = 5.972\ 49$, respectively, is shown in Fig. 4. Corresponding to the CO-CDO transition triggered by the induced disorder, the resistivity has a colossal reduction (indicated as XR process in Fig. 4), as large as four orders of magnitude at low T. Note here that this transition is due to the variation of the charge correlation since no spin correlation is taken into account at all. In addition, an important truth is that the transport behaviors are both insulated irrespective of the fact whether the system is in the CO or CDO states. In the other words, this colossal resistivity reduction corresponds to a nontrivial insulator-to-insulator transition instead of a normal IMT that is often identified in the magnetic framework.

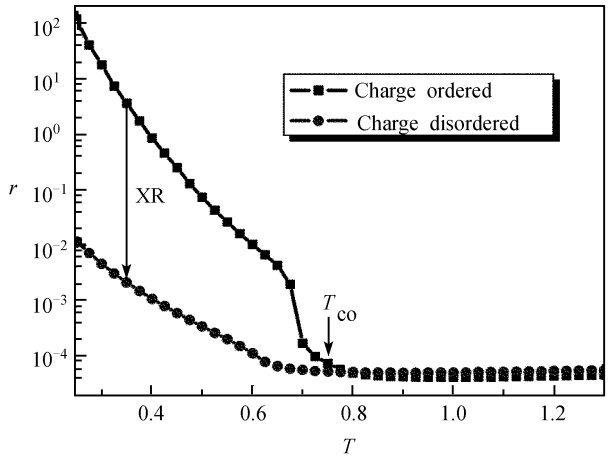

Fig. 4 Simulated resistivity ρ_c as a function of T. When μ_i is homogeneous over the whole lattice, the ground state below T_{CO} is the CO state. As $\sigma^2 = 5.972\ 49$, the CO state is partially suppressed with a dramatic resistivity reduction as big as several orders of magnitudes.

4 Discussions

The simulation presented above allows us to argue that an insulator-to-insulator transition can generate a colossal resistivity change, which is independent of the spin degree of freedom. This transition may be utilized to explain the resistivity reduction in real manganites induced by perturbations other than magnetic field. For instance, it was found that photonic illumination can destabilize the CO state into the CDO state, accompanying the colossal resistivity reduction.

Consequently, we are in a good position to propose a novel framework for the electronic transport in manganites, which can be illustrated schematically with the help of Fig. 5. The red curve represents the ρ - T dependence (CO curve) for a pure CO state in which no contribution from the spin correlation (spin degree of freedom) is included. The blue ρ-T curve (FM curve), which is weakly T-dependent, is for a system offering the PM-FM transitions in the absence of CO state. In fact, it was suggested that there are two kinds of CMR (CMR1 and CMR2) effects [22]. The CMR1 effect is induced by abrupt first-order transitions at low T, such as the CO-CDO transitions. The CMR2 effect, however, refers to the CMR effect that usually appears in the regime around T_C of the PM-FM transitions. In the present framework, the CMR2 process occurs around T_C, as indicated by arrow 1. The MR value is not very large because the FM curve changes smoothly with the T and the PM-FM transitions near T_C being continuous in response to the applied magnetic field. A typical example can be found in $La_{1-x}Sr_xMnO_3$ ($x \sim 0.3$), which is a metal over the whole T range [2].

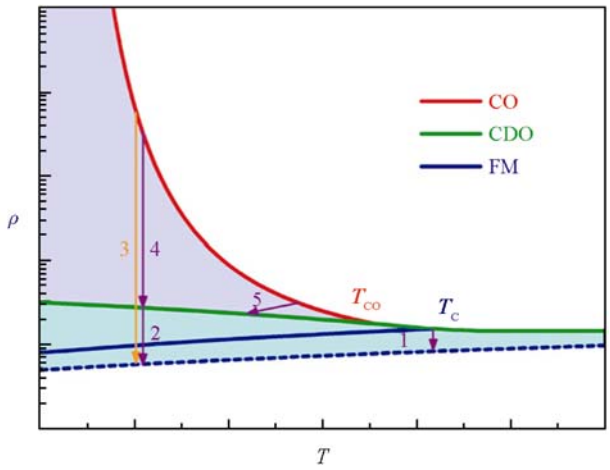

Fig. 5 A schematic of the electronic transport of manganites in the present framework. The T-dependent transport behaviors of charge-ordered (CO) state, charge-disordered (CDO) state and ferromagnetic (FM) state are plotted respectively. The blue dashed curve represents the transport behavior of the FM state under a magnetic field. The vertical axis is resistivity in logarithm scale. The CO state has very poor conductance which decreases rapidly with decreasing T, while the FM state makes the conductance metallic due to the spin-dependent DE mechanism. The CMR2 effect, which is only spin-dependent, is indicated as arrow 1 and arrow 2, while the XR effect, which is only charge-dependent, is indicated as arrow 4. The CMR1 effect, considered as a result of the XR effect plus the CMR2 effect, is shown as arrow 3. The AFM metal is considered as a transition from a weak CO state to a CDO state, as shown by arrows 5. The purple and green regions are dominated by modulations of the charge degree of freedom and spin degree of freedom, respectively. T_C and T_{CO} are the Curie temperature and CO transition temperature, respectively.

The CMR1 effect is a consequence of high-field induced CO-FM transitions at low T, which is different from the CMR2 effect that is indicated by arrow 3. It requires a large critical magnetic field under which a real colossal reduction of resistivity is generated.

In the novel framework proposed here, a CDO state without inclusion of FM ordering is introduced, as indicated by CDO curve. Such a CDO state can be a spin glass or an AFM state of no long-range charge order, which was observed in $La_{0.23}Ca_{0.77}MnO_3$ [31]. The zero-field ground CDO state is an insulator, but its resistivity has a milder T-dependence than the pure CO states. Consequently, the resistivity at low T is at least a few orders of magnitude lower than that of the CO states. The CDO state can be classified as a "bad" insulator. The transport behavior of $Pr_{0.5}Sr_{0.5}MnO_3$ (no clear CO sign from neutron diffraction)

below the Neel point T_N (AFM, $T_N \sim 150$ K) [30] can be considered as an example of the CDO curve. The CDO state is an important ingredient to understand the X-induced resistivity change (we call it XR), in this situation X may be any physical process such as photon illumination, pressure, electric current, and so on. The X process may melt the CO state into the CDO state without much change in the spin correlation [19]. As shown in Fig. 6, the periodic charge density in the CO states, or periodic coulomb repulsion, is absent in the CDO states, in which most Mn cations have the average e_g electron density. It is favored for carriers to move in a relatively leveled potential background. The conductiveity is largely enhanced (several orders of magnitude) in the CO-CDO transition, as indicated by arrow 4 in Fig. 5. Furthermore, the CDO state can be easily transferred to FM state, because the resistivity does not change much for the transition of "bad" insulator to "bad" metal. This CDO-FM transition may be triggered by a spin-dependent DE-mediated process, and thus it can be classified as a CMR2 effect (arrow 2). Although the CO states are stable against magnetic field or pressure below the threshold, they are sensitive to the site disorder, because of the cooperative lattice effect [8]. Local illumination [14—17] may have the same effect as local site disorder. It was demonstrated [14, 15] that illumination may even cause the IMT process rather than the XR sequence, because the DE sequence cannot be avoided in these manganites.

The above scenario can also be applied to explain those observed phenomena but not yet well understood in manganites. The AFM metallic behavior in some manganites is hard to explain in the magnetic framework. It actually corresponds to a transition of a weak CO state to a CDO state of the AFM order upon decreasing T, as indicated by arrow 5 in Fig. 5. If we extend the definition of the CMR1 effect to the sequence indicated by arrow 3 in Fig. 5, the CMR1 effect can be understood as two sequences: the CO state is melted into the CDO state, followed by the CDO-FM transitions. Thus, one has CMR1 = XR + CMR2 with XR $\gg$ CMR2, although the XR effect is an insulator-to-insulator transition rather than an IMT. This partition of the CMR1 effect into two sequences is not trivial, and it highlights some possibilities for potential applications of manganites, in which one may utilize the XR effect rather than the CMR (so as IMT), because the intrinsic large magnetic field required for CMR effect and imbalance between high T_C and large MR make magnetic applications of manganites hard to break through. The XR effect can be achieved simply by photo- illumination or other process.

Finally, we have to mention that the true CO configuration in manganites (checkerboard arrangement in x-y plane and charge-stacking along z axis) cannot be stable without AFM super exchange between the NN t_{2g} spins. The CO configuration studied in this situation is the electron Wigner crystal since we exclude the spin correlation (spin degree of freedom). In fact, electron Wigner crystal is also a CO state, which was once used by Goodenough in early days of manganites research [33], although it is different from the true CO structure of real manganites. We use this toy model instead of real manganites in the present work, for the reasons that the colossal XR effect has no relation with the spin correlation, and the difference in resistivity between the real CO states and the Wigner CO state is not dominant. Besides, this toy model can predict the property of the pure CO/CDO transitions, which cannot be reached with real manganites, where the spin correlations make the problem extremely complex.

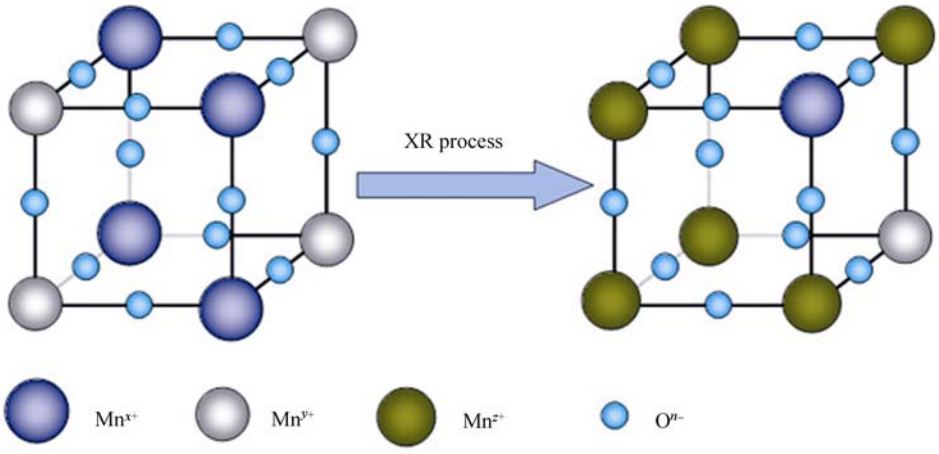

Fig. 6 An example of the XR effect due to the CO-CDO transition. Here the arrangement of e_g electrons in the CO state favors a charge stacking configuration rather than a Wigner crystal. In the CDO state shown here, most Mn cations are Mn^{z+}, which have the averaged e_g electron density. The periodic charge density in the CO states, or periodic coulomb repulsion, is absent in the CDO states. Then it is advantaged for carriers to move in a relatively leveled potential background and the conductivity is largely increased in the CO-CDO transition. Here Mn^{x+}, Mn^{y+}, Mn^{z+} and O^{n-} are Mn^{3+}, Mn^{4+}, $Mn^{3.5+}$ and O^{2-} respectively in common knowledge. Recently, it is argued that the valences of Mn and O ions in real CO states are more complex [32]. However, it does not affect this framework because the period of charge density still exists although $y - x \neq 1$.

5 Conclusions

In summary, several major issues as revealed by extensive experimental investigations on the transport properties of manganites cannot be reasonably understood in the magnetic framework. We have highlighted the main problems that need to be solved. A novel framework has been proposed, in which the total resistivity of manganites has been separated into two parts, i.e., spin-dependent term ρ_s and charge-dependent term ρ_c. The charge degree of freedom as an essential source to modulate the transport behaviors of manganites is particularly emphasized. The novel framework has been successfully applied to explain a series of very scattered transport behaviors observed in different manganites, which offer various combinations of the charge degree of freedom and spin degree of freedom.

Acknowledgements We thank E. Dagotto for comments and suggestion. Dong S. thanks Dai S. for assistance. This work was supported by the National Natural Science Foundation of China (Grant Nos.50332020, 10021001) and the National Key Projects for Basic Research of China (Grant Nos. 2002CB613303, 2004CB619004).

References

1. For a review, see: Dagotto E., Nanoscale Phase Separation and Colossal Magnetoresistance, Springer-Verlag, Berlin, 2002
2. Uehara M., Mori S., Chen C H, and Cheong S. -W., Percolative phase separation underlies colossal magnetoresistance in mixed-valent- manganites, Nature, 1999, 399: 560－563
3. Zhang L. et al., Direct observation of percolation in a manganite thin film, Science, 2002, 298: 805－807
4. Tokunaga M., Tokunaga Y., and Tamegai T., Imaging of percolative conduction paths and their breakdown in phase-separated $(La_{1-y}Pr_y)_{0.7}Ca_{0.3}MnO_3$ with $y = 0.7$, Phys. Rev. Lett. 2004, 93: 037203
5. Moreo A., Yunoki S., and Dagotto E., Phase separation scenario for manganese oxides and related materials, Science, 1999, 283: 2034－2040
6. Mayr M. et al., Resistivity of Mixed-phase manganites, Phys. Rev. Lett., 2001, 86: 135－138
7. Burgy J., Moreo A., and Dagotto E., Relevance of cooperative lattice effects and stress fields in phase-separation theories for CMR manganites, Phys. Rev. Lett., 2004, 92: 097202
8. Kumar S. and Majumdar P., Nanoscale phase coexistence and percolative quantum transport, Phys. Rev. Lett., 2004, 92: 126602
9. Dong S., Zhu H., Wu X., and Liu J.-M., Microscopic simulation of the percolation of manganites, Appl. Phys. Lett. 2005, 86: 022501
10. Dong S., Yao X. -Y., Wang K.-F., and Liu J.-M., Phase equilibrium in manganites under a magnetic field studied using a two-orbital model, J. Phys.: Condens. Matter, 2006, 18: L171－L177
11. Tomioka Y., Asamitsu A., Kuwahara H., Moritomo Y., and Tokura Y., Magnetic-field-induced metal-insulator phenomena in $Pr_{1-x}Ca_xMnO_3$ with controlled charge-ordering instability, Phys. Rev. B, 1996, 53: R1689－R1692
12. Okimoto Y., Tomioka Y., Onose Y., Otsuka Y., and Tokura Y., Optical study of $Pr_{1-x}Ca_xMnO_3$ (x=0.4) in a magnetic field: Variation of electronic structure with charge ordering and disordering phase transitions, Phys. Rev. B, 1999, 59: 7401－7408
13. Hwang H. -Y., Cheong S.-W., Ong N.–P., and Batlogg B., Spin-polarized intergrain tunneling in $La_{2/3}Sr_{1/3}MnO_3$, Phys. Rev. Lett., 1996, 77: 2041－2044
14. Kiryukhin V. et al., An X-ray-induced insulator metal transition in a magnetoresistive manganites, Nature, 1997, 386: 813－815
15. Fiebig M, Miyano K, Tomioka Y, and Tokura Y, Visualization of the local insulator-metal transition in $Pr_{0.7}Ca_{0.3}MnO_3$, Science, 1998, 280; 1925－1928
16. Miyano K., Tanaka T., Tomioka Y., and Tokura Y., Photoinduced insulator-to-metal transition in a perovskite manganite, Phys. Rev. Lett., 1997, 78: 4257－4260
17. Smolyaninova V. N. et al., Photoinduced resistivity changes in $Bi_{0.4}Ca_{0.6}MnO_3$ thin films, Appl. Phys. Lett., 2005, 86: 071922
18. Asamitsu A., Tomioka Y., Kuwahara H., and Tokura Y., Current switching of resistive states in magnetoresistive manganites, Nature, 1997, 388: 50－52
19. Zhao Y. -G. et al., Universal behavior of giant electroresistance in epitaxial $La_{0.67}Ca_{0.33}MnO_3$ thin films. Appl. Phys. Lett., 2005, 86: 122502
20. Moritomo Y., Kuwahara H., Tomioka Y., and Tokura Y., Pressure effects on charge-ordering transitions in perovskite manganites, Phys. Rev. B, 1997, 55: 7549－7556
21. Cui C., Tyson T. A., Chen Z., and Zhong Z., Transport and structural study of pressure-induced magnetic states in $Nd_{0.55}Sr_{0.45}MnO_3$ and $Nd_{0.5}Sr_{0.5}MnO_3$, Phys. Rev. B, 2003, 68: 214417
22. Aliaga H. et al., Theoretical study of half-doped models for manganites: Fragility of CE phase with disorder, two types of colossal magnetoresistance, and charge-ordered states for electron-doped materials, Phy. Rev. B, 2003, 68: 104405
23. Motome Y., Furukawa N., and Nagaosa N., Competing orders and disorder-induced insulator to metal transition in manganites, Phys. Rev. Lett., 2003, 91: 167204
24. Şen C., Alvarez G., and Dagotto E., Insulator-to-metal transition induced by disorder in a model for manganites, Phys. Rev. B, 2004, 70: 064428
25. Rama N. et al., A-site-disorder-dependent percolative transport and Griffiths phase in doped manganites, Phys. Rev. B 2004, 70: 224424
26. Wang K.-F. et al., Ferromagnetic metal to cluster-glass insulator transition induced by A-site disorder in manganites, Appl. Phys. Lett. 2006, 88: 152505
27. Wang K. -F. et al., Cluster-glass state in manganites induced by A-site cation-size disorder, Phys. Rev. B, 2006, 73: 134411
28. Akimoto T. et al., Antiferromagnetic metallic state in doped manganites, Phys. Rev. B, 1998, 57: R5594－R5597
29. Yoshizawa H., Kawano H., Fernandez-Baca J. A., Kuwahara H., and Tokura Y., Anisotropic spin waves in a metallic antiferromagnet $Nd_{0.45}Sr_{0.55}MnO_3$, Phys. Rev. B, 1998, 58: R571－R574
30. Kawano H. et al., Magnetic ordering and relation to the metal-insulator transition in $Pr_{1-x}Sr_xMnO_3$ and $Nd_{1-x}Sr_xMnO_3$ with $x \sim 1/2$, Phys. Rev. Lett., 1997, 78: 4253－4256
31. Tao J., Niebieskikwiat D., Salamon M. B., and Zuo J. -M., Lamellar Phase Separation and Dynamic Competition in $La_{0.23}Ca_{0.77}MnO_3$, Phys. Rev. Lett., 2005, 94: 147206
32. Coey M., Charge-ordering in oxides, Nature, 2004, 430: 155–156
33. Goodenough J. B., Theory of the role of covalence in the perovskite-type manganites [La, M(II)] MnO_3, Phys. Rev., 1995, 100: 564－573